JMEPEG (2011) 20:147–154
DOI: 10.1007/s11665-010-9657-6

1059-9495/$19.00

Plate Thickness Variation Effects on Crack Growth Rates in 7050-T7451 Alloy Thick Plate

Joel J. Schubbe

(Submitted December 23, 2009; in revised form March 16, 2010)

A study has been accomplished to characterize the fatigue crack growth rates and mechanisms in thick plate (16.51 cm) commercial grade 7050-T7451 aluminum plate in the L-S orientation. Examination of the effects of potential property gradients in the plate material was accomplished through hardness measurements along the short transverse direction and with compact tension tests. Tests exhibited a distinct trend of reduced center plane hardness in the plates. Compact tension specimens and the compliance method were used to determine crack growth rates for specimens machined from the t/4 and t/2 planar locations and oriented for L-S crack growth. Crack growth rate data (long crack) from the tests highlighted significant growth rate differences between the t/4 and t/2 locations. No significant effect of *R*-ratio was observed in the 0.05-0.3 range tested. Additionally, crack front splitting was noted in all specimens to differing degrees with data showing significant retardation of growth rate curves for the L-S orientation above 13 MPa √m in the center plane, and 10 MPa √m at quarter plane, where branching and splitting parallel to the load axis are dominant growth mechanisms.

Keywords aerospace vehicles, aluminum alloys, delamination, fatigue crack growth, fractography, fracture mechanics, mixed mode fracture

1. Introduction

The 7050-T7451 aluminum alloy system is used extensively in both military and commercial aircraft systems due to its advertised strength characteristics and corrosion-resistant characteristics (Ref 1). The rolled and heat-treated nature of this plate alloy creates a material that is highly anisotropic in nature and must be fully tested with the range of loads representative of those expected in service. The most common orientations' strength properties are well characterized, but if experimental crack growth rate data and fatigue properties for the L-S orientation are to be used for life estimates, they have not been tested at sufficient levels for these predictions. Common practice is to use available data for L-T or T-L orientations when L-S data are not available. Previous studies show the significant differences in crack growth rates and growth mechanisms for this substitution. (Ref 2, 3). Fatigue growth rates for most other orientations have been characterized by manufacturers or users in the aerospace community (Ref 4-6). This study was initiated to examine potential gradients in material properties that would be exhibited as the plate product used for component parts increased in thickness. The intent of using a thick plate product in lieu of a built-up part or deep forging is to reduce overall weight or to avoid significant residual stresses and potential warping in final machining processes. It should be noted that the testing accomplished requires a minimum thickness plate to achieve sufficient size compact tension specimens at multiple planar locations, in this study specimens centered at t/2 and t/4 were chosen for testing and examination. All specimens in this study were etched using a Keller's Reagent solution. Figure 1 shows the morphology of mid-plane grain structure for the 16.51 cm plate thickness. It should be noted that the mid-plane aspect ratio of the 16.51 cm plate product is 20% lower in the L-S orientation than was previously observed in the 10.16 plate shown in the previous study (Ref 3).

Joel J. Schubbe, Mechanical Engineering Department, US Naval Academy, 590 Holloway Road, Annapolis, MD 21402. Contact e-mail: Schubbe@usna.edu.

2. Experimental Methodology

2.1 Specimens and Test Setup

Specimens tested in this study were cut from a 7050-T7451 aluminum plate of parent thickness 16.51 cm. The list of specimens in this study is in Table 1 and orientations for L-T, T-L, and L-S are shown in Fig. 2. ASTM E647 standards for fatigue crack growth testing were followed to configure and prepare the pin-loaded compact tension (CT) specimens for testing to generate data and were configured as in Fig. 3 (Ref 7) and 4. L-S specimens were tested exclusively in this study and compared to data from previous L-S data generated from 10.16 cm plate specimens. The L-S oriented specimens were tested to generate da/dN versus ΔK long crack growth data plots and examine the influence of plate thickness and planar location on the mechanisms associated with the material crack morphology seen in 10.16 plate specimens. Testing in an approximate range of 5-35 MPa √m was accomplished at 10 Hz and at load ratios of $R = 0.05$, 0.1, and 0.3. A minimum of three repeat tests for each load ratio and at each planar location were accomplished to examine repeatability and to compare the t/2 and t/4 data.

A MTS 810 electric servo-hydraulic 22kip test stand was used to pin load the specimens, and control was accomplished using an external MTS Flex SE Test controller with MTS PC interface software. Load considerations included the load ratio, thickness to specimen depth, K-gradients, and maintaining a small-scale yielding criteria. Tests were conducted in a tension-tension mode due to specimen type and Cyctest software was used to regulate the growth loads and gradients of continuous load shedding during test. Cycle by cycle feedback was provided to enable real-time load corrections. In addition, crack-tip opening displacement (CTOD) data from the MTS clip gage was recorded and used within the Cyctest software program to determine crack growth rates using the crack

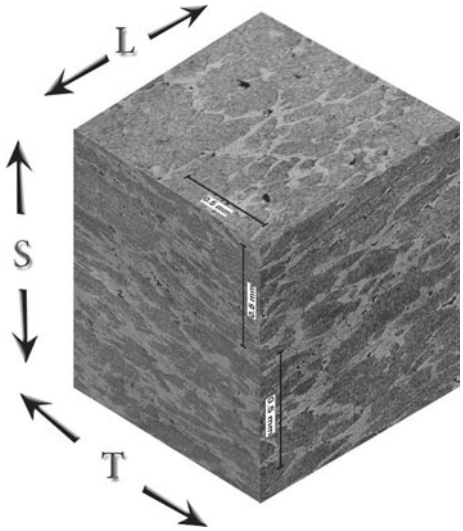

Fig. 1 16.51 cm Plate (t/2 plane)

Table 1 Specimen listing

Plate thickness, cm	*R*-ratio	Orientation	Plane
16.51	0.3	L-S	t/4
16.51	0.3	L-S	t/4
16.51	0.3	L-S	t/4
16.51	0.1	L-S	t/4
16.51	0.1	L-S	t/4
16.51	0.1	L-S	t/4
16.51	0.05	L-S	t/4
16.51	0.05	L-S	t/4
16.51	0.05	L-S	t/4
16.51	0.05	L-S	t/4
16.51	0.3	L-S	t/2
16.51	0.3	L-S	t/2
16.51	0.3	L-S	t/2
16.51	0.3	L-S	t/2
16.51	0.1	L-S	t/2
16.51	0.1	L-S	t/2
16.51	0.1	L-S	t/2
16.51	0.05	L-S	t/2
16.51	0.05	L-S	t/2
16.51	0.05	L-S	t/2

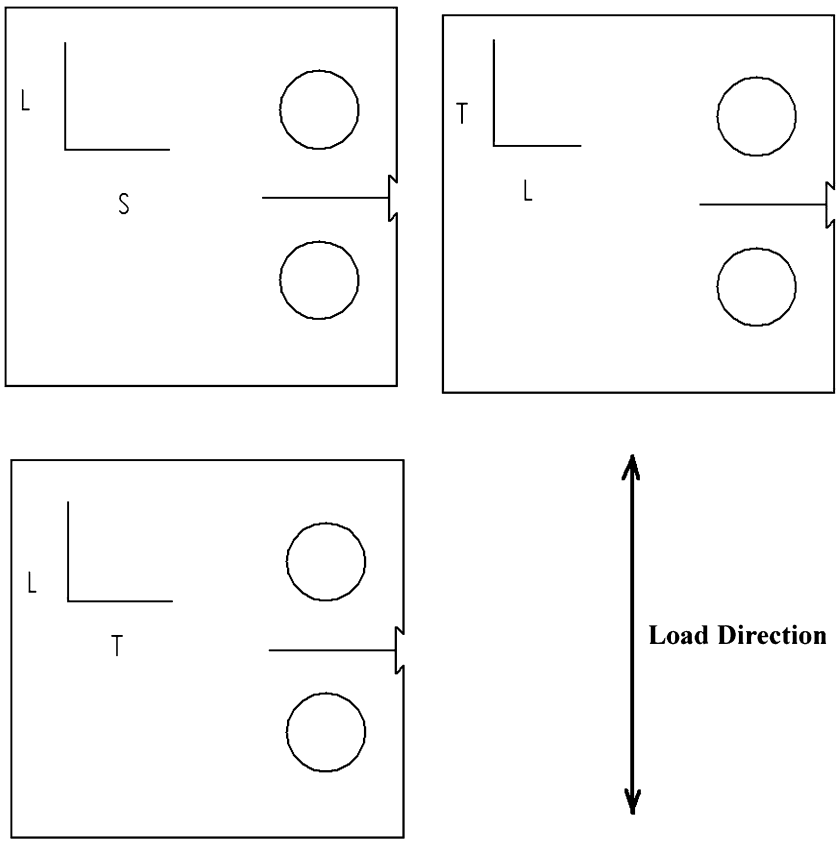

Fig. 2 Specimen orientation

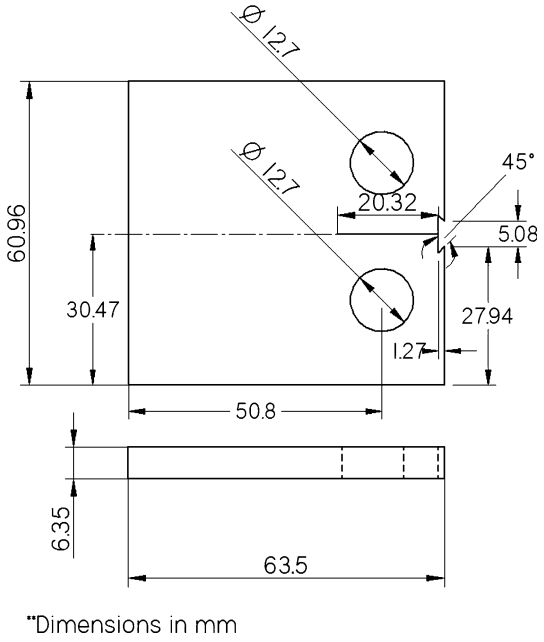

Fig. 3 Specimen configuration

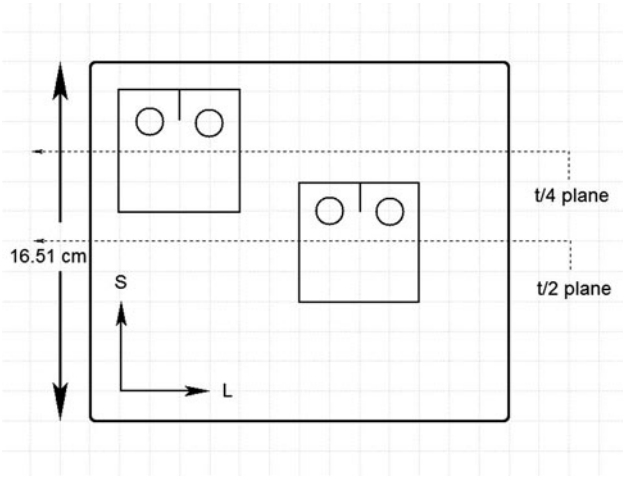

Fig. 4 Specimen fabrication locations

closure compliance method. Optical checks were performed to guarantee the crack length accuracy being used for compliance calculations during test. Crack lengths recorded using the compliance method were validated using a Gaertner traveling optical telemicroscope with digital readout.

Specimens were electro-discharge machined (EDM) with integral knife edges to allow for the MTS gauge placement and 0.254 mm notch for crack initiation. The surface finish of the specimens from machining met a requirement of RHR < 25 and then was minimally hand-polished to allow better visualization of the crack by telemicroscope. Pre-cracking was accomplished at a ΔK of 8.8 MPa $\sqrt{m}$ at 10 Hz to a length sufficient to eliminate effects of the machined notch according to ASTM E647 and the range of testing was accomplished through decreasing or increasing ΔK with ASTM standard gradients.

3. Results and Discussion

3.1 Hardness Gradient Measurement

Initial supposition for this study described a potential gradient of material properties, likely affecting crack growth, was due to a manufacturing process, to include rolling or heat treatment of the alloy system. This gradient may become more pronounced with increasing thickness of material and could show itself with residual stresses due to rolling processes and resultant changes in localized tensile yield stress and exhibited by hardness measurements of the material. These increases in hardness are empirically correlated to localized yield stress, as shown by standardized Rockwell hardness scales. In addition, these hot rolling processes can result in a composition and structure gradient that will affect hardness and localized yield stress due to constituent particle size, orientation, and concentrations. Alcoa detailed these properties evidenced by microstructural gradients and constituents at the t/10, t/4, and t/2 planes; all of which were exhibited and quantified due to cooling gradients and rolling method (Ref 8). Alcoa also observed little influence of porosity on final rolled plate product morphology (aspect ratio 0.51 versus 0.52 for standard versus low porosity plate). Sample plates (16.51 and 10.16 cm) of material were cut in the L-S orientation and Rockwell B hardness measurements were taken in equally spaced bin distances across the short transverse direction to provide insight to residual stress or related tensile strength variations from surface-to-surface of each plate. It is this relationship between hardness and ultimate tensile strength or yield strength that provides a qualitative insight to the resulting crack growth rates. Each location data point is a compilation and average of a minimum of three tests. Though not directly related to residual strength, the Rockwell B hardness test can show relative property changes or gradients through the thickness of the parent plate product from which these specimens were fabricated. Figure 5 shows the trend results of the hardness measurements normalized to the "near-surface" bin values (t/10). Polynomial fits are provided for trend visualization only. Horizontal axis values are normalized to distance through each plate and therefore 0.5 is equivalent to the t/2 plane of each plate. Rockwell B hardness measurements provided a raw near-surface bin value averaging approximately 87 for both plate thicknesses. The normalized variation from near-surface to centerline varies in the range of 0.5-2.0%, relative to front side measurements and reflects property changes through the thickness of the plate. The affected properties are likely attributable to the rolling processes and/or the heat treatment of the 7050-T7451 product. Centerline cooling rates may also contribute to grain and constituent concentration and morphology. The 16.51 cm plate shown in this study can be compared to the morphology of the slow cooled 7050 alloy detailed by Robson (Ref 9). Additional residual stress or material tests would be required to specify the direct causes. It is clear, however, that a surface applied process has affected the grain structure and properties through the thickness of each plate, with a larger gradient present in the 10.16 plate product. Figure 6 shows a t/4 versus t/2 direct comparison of grain structure with decreased t/2 grain aspect ratio. An example of where this change may affect design should be examined for a deep frame with flange in the L-T orientation and transitioning to L-S orientation, properties changing from flange tip to shear web-interface, and shear web

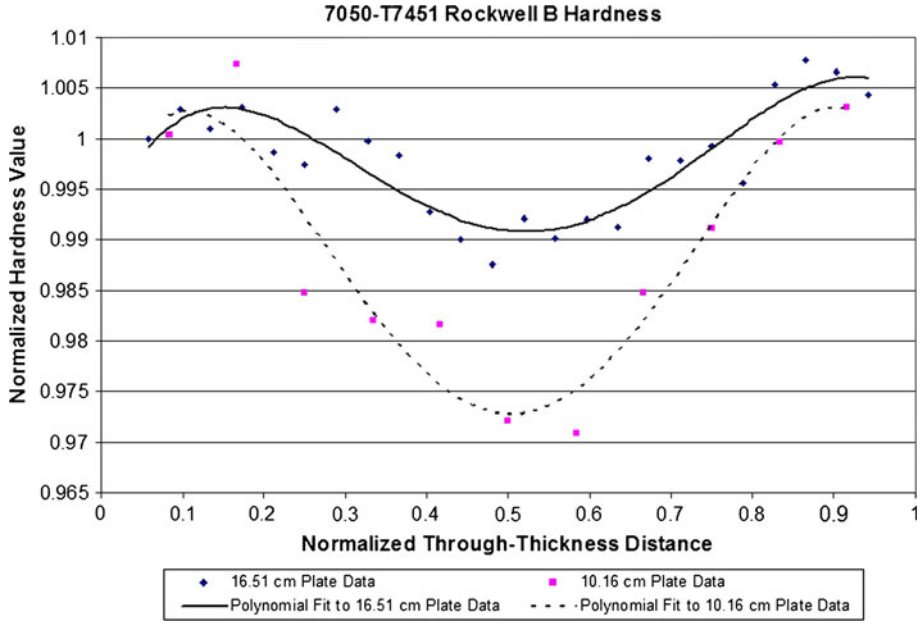

Fig. 5 Normalized hardness measurements (through short-transverse)

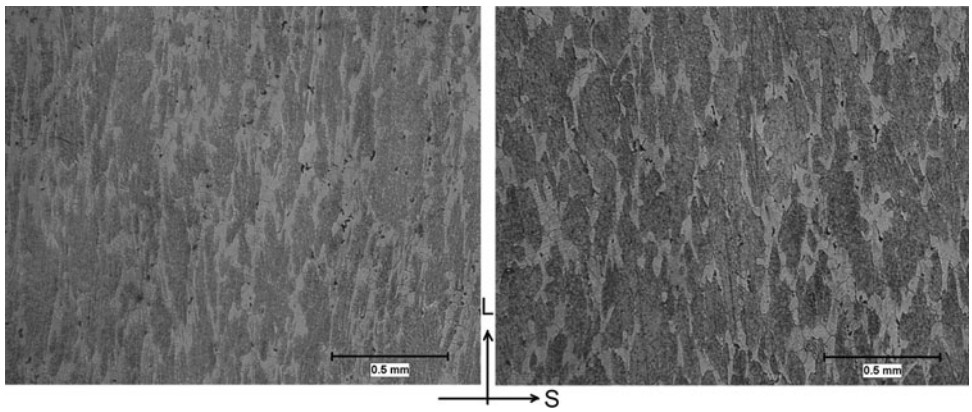

Fig. 6 L-S grain comparison (t/4—left vs. t/2—right)

properties associated with the decreased tensile strengths of the centerline thick plate values.

3.2 Growth Rates

3.2.1 Crack Growth Measurement. Previous studies provided initial comparisons of ΔK versus crack growth rate tests performed on thin (1.27 cm) and thick (10.16 cm) parent material in the L-T and T-L orientations (Ref 2, 3). More importantly these studies provided L-S crack growth rate comparison data for 10.16 cm plate product. Figure 7 displays comparison data from centerline of the 10.16 cm plate. Additionally, centerline data for the L-T and T-L orientations in the 10.16 cm plate are shown for reference. It should be noted that in each L-S case shown, the crack splitting and meandering became a dominant growth mechanism at the 13-15 MPa $\sqrt{m}$ stress range level. This trend is evident in each growth rate plot found in this study by a distinct drop in main crack forward growth rate. As dominant growth progresses in the L-orientation (parallel to load), forward growth measured by the crack opening/compliance method decreases and is no longer meaningful to single crack life predictions.

A compilation of data from the 16.51 cm plate testing is shown in Fig. 8. The figure is shown to display the overall grouping of data for the 16.51 cm plate thickness. Later, Fig. 9-11 shows a breakout of the data comparing *R*-ratio (0.05, 0.1, and 0.3) and planar location (t/2, t/4). The divergence of the curves for all *R*-ratios between the t/2 and the t/4 data begins at approximately 10 MPa $\sqrt{m}$ and is clearly distinguishable. The forward main crack growth rate in the t/2 plane specimens is consistently greater, by nearly two to three times, relative to the t/4 plane. It can be surmised that the apparent slowed growth and splitting or meandering of the crack is less in the mid-plane (t/2) specimens than in the quarter plane (t/4) specimens nearer the surface. Near the surface, the grain structure is more anisotropic due to grain morphology (higher

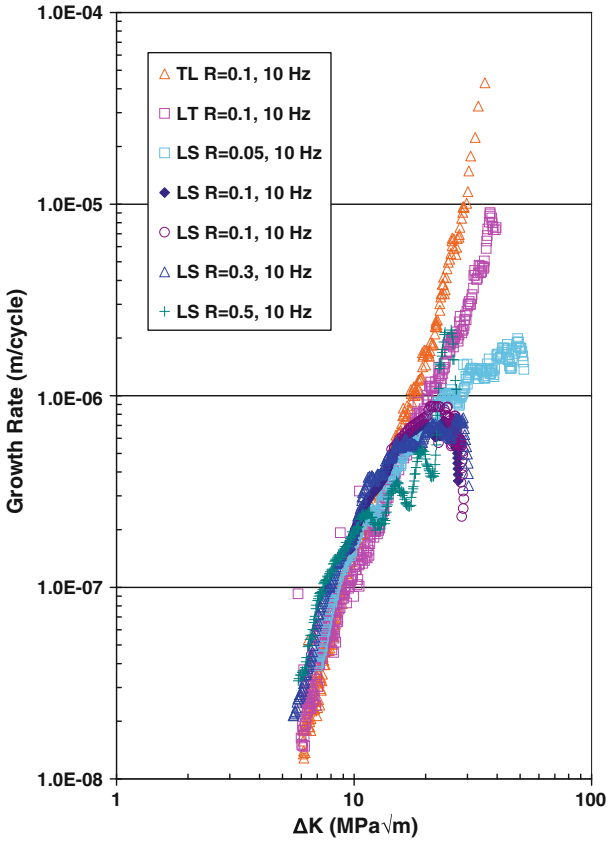

Fig. 7 10.16 cm Plate crack growth data

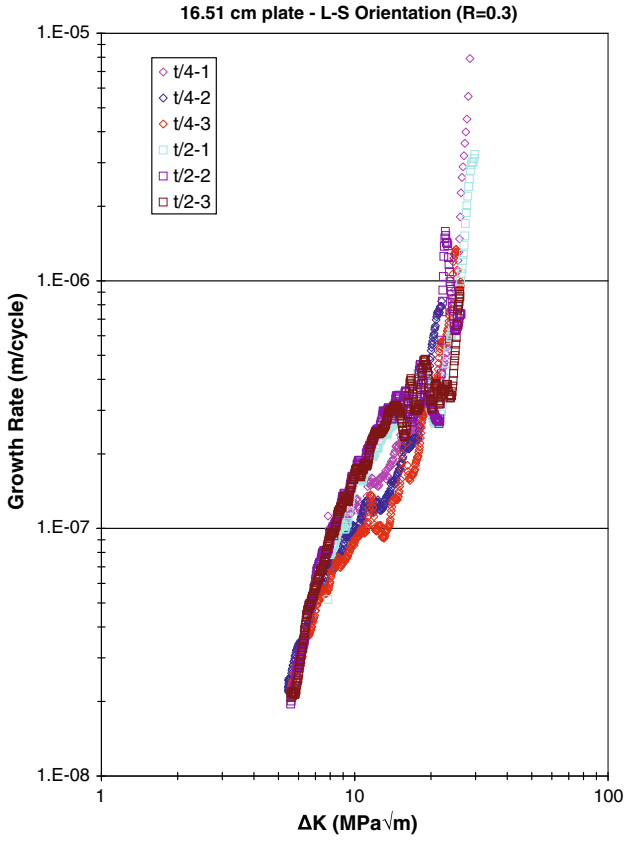

Fig. 9 T/4 and T/2 comparison at $R = 0.3$

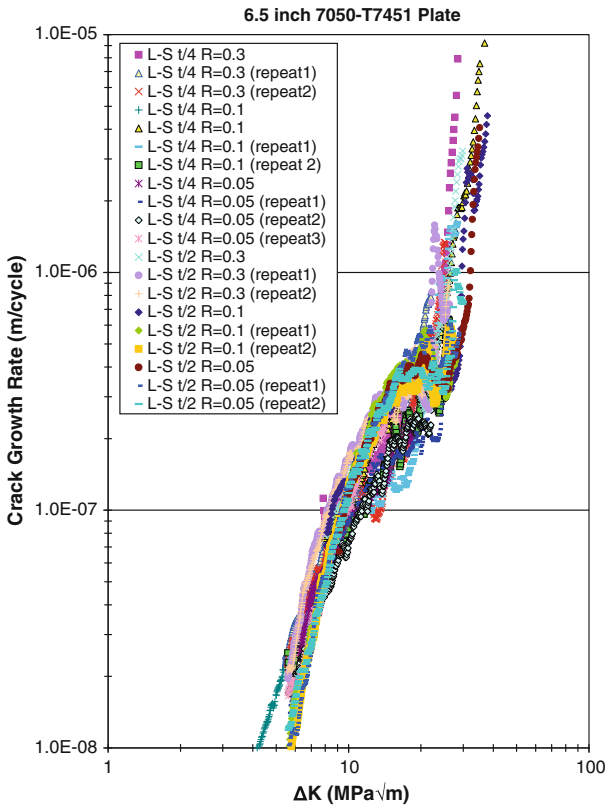

Fig. 8 7050-T7451 L-S data compilation

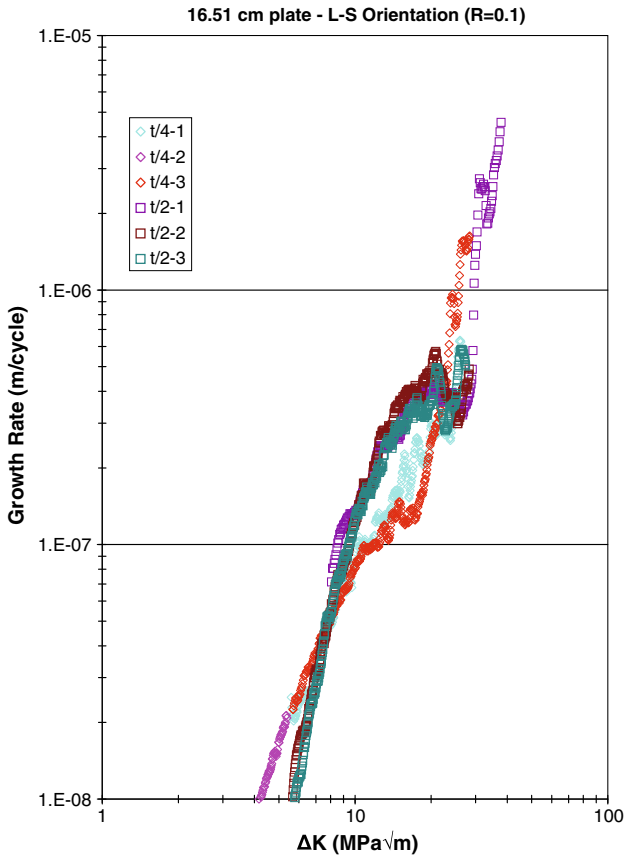

Fig. 10 T/4 and T/2 comparison at $R = 0.1$

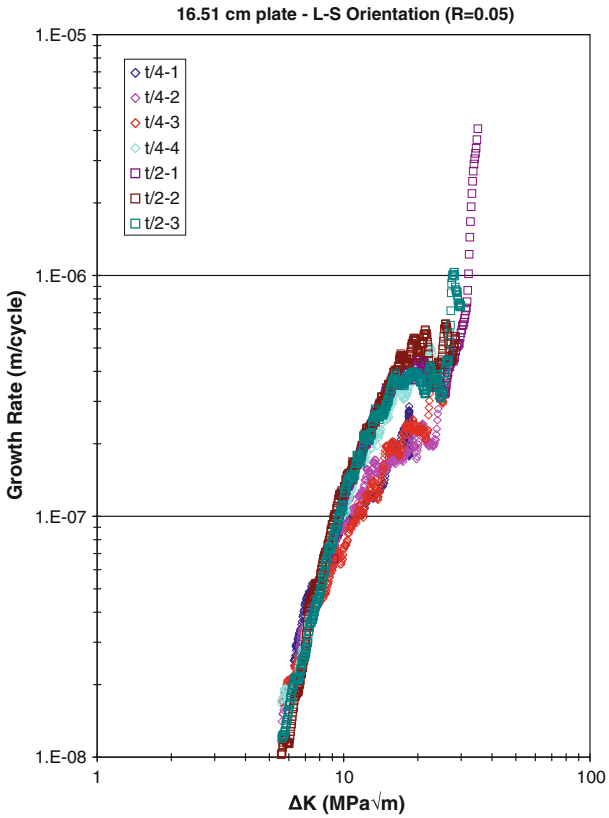

Fig. 11 T/4 and T/2 comparison at $R = 0.05$

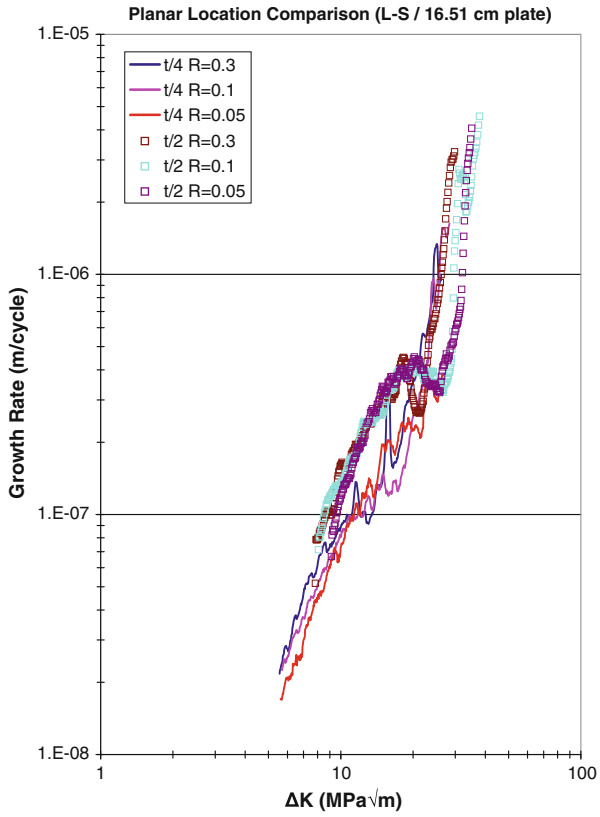

Fig. 12 Comparison of T/4 and T/2 at stress range levels $R = 0.3$, 0.1, 0.05

aspect ratio grain structure) and greater hardness (residual stresses). Both planes exhibit significant retardation of forward growth beginning in the 15-18 MPa √m range, similar to the thinner (10.16 cm) plate material, and consistent with previous experimental data (Ref 2). Consolidated data for each of the *R*-ratio data sets (Fig. 12) show little dependence on *R*-ratio and a significant dependence on planar location. This data set demonstrates that material property changes from the outer surface to the inner planes have a notable influence on growth rate for these specimens.

Figure 13 shows a comparison of selected 10.16 cm plate data (Ref 2) with a representative set of data from the 16.51 cm plate testing. Since t/4 plane specimens in this configuration cannot be fabricated from the 10.16 cm plate in the short transverse direction, there is no data to compare for the 10.16 cm t/4 plane. L-T and T-L data are included for the 10.16 cm plate for comparison. It was observed that the centerline (t/2) growth data in the 16.51 and 10.16 cm plates more closely aligns with the centerline (t/2) 10.16 cm L-T data and that there is a notable difference of crack growth rates due to additional splitting and retardation for the t/4 plane specimens. The standard practice of substituting L-T data for unavailable L-S data comes into question for parts such as aerospace frames and spars which may undergo grain orientation changes relative to loading throughout the flange. The trends of the L-S orientation data show a divergence of all data from the L-T data set due to splitting/meandering at approximately 15 MPa √m. Even earlier divergence is seen for the t/4 plane at around 10 MPa √m. This t/4 planar location could potentially coincide with the location of flange fastener holes,

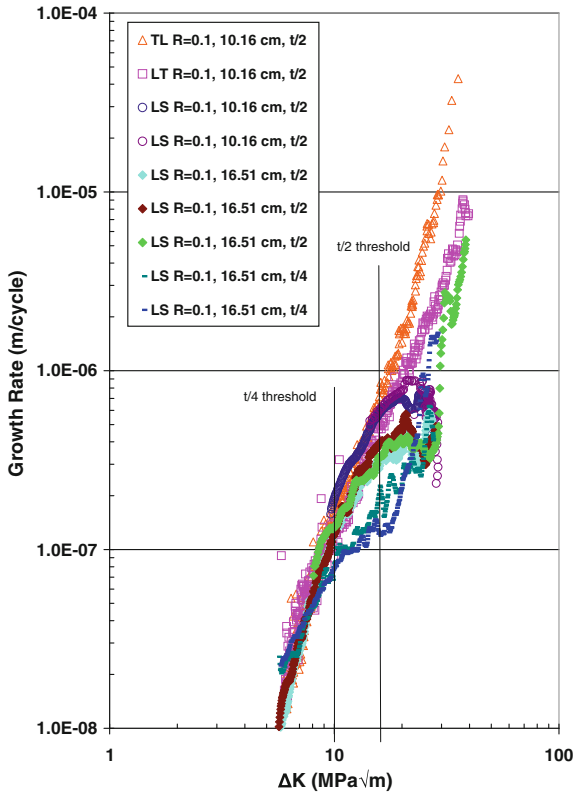

Fig. 13 Comparison of 16.51 cm plate to 10.16 cm plate data

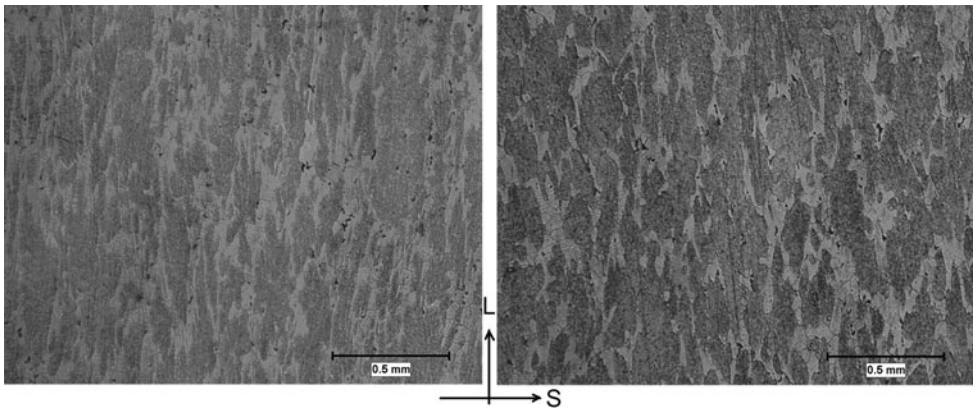

Fig. 14 L-S Grain structure (t/4—left, t/2—right)

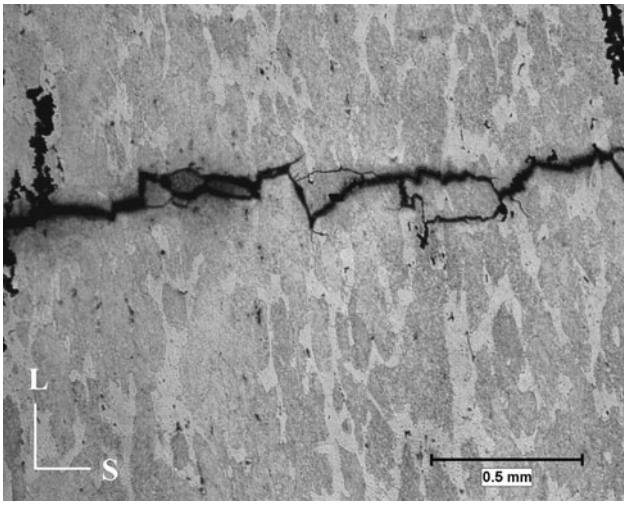

Fig. 15 t/2 Crack progression (left to right)

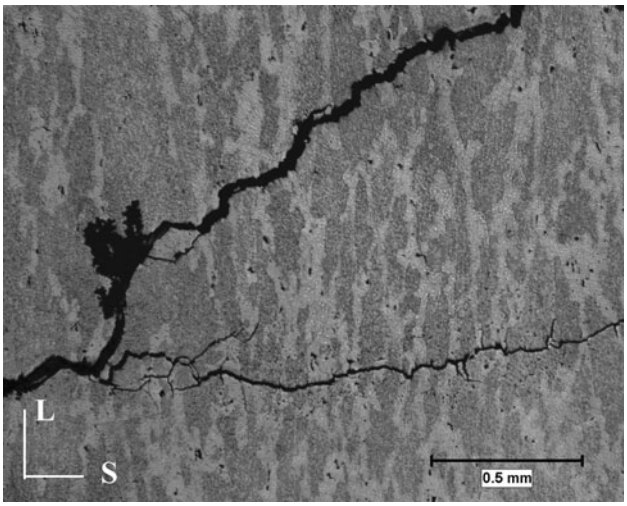

Fig. 16 t/4 Crack progression (left to right)

transition features or even the shear web-flange interfaces, creating the potential of crack turning, splitting, or unpredictable reorientation of growth in the presence of existing crack growth.

Fig. 17 L-S oriented splitting in 1.27 cm L-T specimen

3.3 Crack Front Morphology

The forward growth of L-S cracking in this plate product is intergranular in nature and is also dominated by the splitting of grain boundaries in the direction perpendicular to the main crack growth. Thus, the crack is turned or branches on a continual basis once the crack is long. The crack progression rate is slowed by the energy diverted to multiple crack growth or perpendicular growth but eventually the primary forward progression dominates and continues forward-oriented cracking. The differences in growth between the t/4 and t/2 planar specimens appear to be characterized by the differences in grain structure between the two. Figure 14 shows the differences in heterogeneity and grain aspect ratio between the two planes. As shown in Fig. 15 and 16, growth in the t/2 plane, though exhibiting the characteristic splitting, perpendicular growth, tends to be less distinct because of the wider grain sizes. The t/4 plane specimens show the splitting mechanism earlier (shorter crack/lower stress levels) and is more distinctly perpendicular as the grain boundaries are more defined in that direction. The crack direction results in rate reduction of forward growth in the t/4 planar location and a lower stress range threshold at which the phenomenon occurs. Newman et al. (Ref 10) noted a similar splitting mechanism (Fig. 17) in the fast growth region of 1.27 cm L-T oriented plate specimens. These splits were oriented the same as the L-S specimen splitting.

4. Summary

Test results for this study of 7050-T7451 specimens showed that there is a definitive crack growth property gradient through the thickness of plate products and that the growth rates can differ as much as three times from t/4 to t/2 planar location in the 16.51 cm plate. Crack splitting and meandering, occurring throughout this plate product, is associated with forward main crack growth rate reduction and is increased at the t/4 location in the product. Hardness measurements indicate potential high-gradient residual stresses or localized yield stress variation near the surface of the thick plate product. This environment, in addition to high-aspect ratio grain structure, potentially increases these splitting and meandering effects.

Acknowledgments

This work was supported by the US Navy, the US Air Force, and their respective laboratories. Special thanks to USN LTs Ethan Lust and Paul Coco for joining in the exploration of material characterization.

References

1. J. Branger, Life Estimation and Prediction of Fighter Aircraft, *Proceedings of International Conference on Structural Safety and Reliability*, Pergamon Press, New York, 1972, p 213–237
2. J. Schubbe, Evaluation of Fatigue Life and Crack Growth Rates in 7050-T7451 Aluminum Plate for T-L and L-S Oriented Failure Under Truncated Spectra Loading, *Eng. Fail. Anal.*, 2009, **16**, p 340–349. doi: 10.1016/j.engfailanal.2008.05.009
3. J. Schubbe, Fatigue Crack Propagation in 7050-T7451 Plate Alloy, *Eng. Fract. Mech.*, 2009, **76**, p 1037–1048. doi:10.1016/j.engfracmech.2009.01.006
4. Alcoa—Product Catalog: 7050 Aluminum Alloy Plate and Sheet, 2007
5. Metals Handbook, *Vol 2 - Properties and Selection: Nonferrous Alloys and Special-Purpose Materials*, ASM International, 10th edn., 1990
6. Kaiser Aluminum—Technical Reference Library: Alloy 7050, 2007
7. ASM Handbook, *Volume 19, Fatigue and Fracture*, ASM International, 1996, p 170–176
8. J.R. Brockenbrough, R.J. Bucci, A.J. Hinkle, J. Liu, P.E. Magnusen, and S.M. Miyasato, Role of Microstructure on Fatigue Durability of Aluminum Aircraft Alloys, Alcoa Technical Center, Quarterly Report, 15 October 1993, Contract no. N00014-91-C-0128
9. J.D. Robson, Microstructural Evolution in Aluminum Alloy 7050 During Processing, *Mater. Sci. Eng. A*, 2004, **382**, p 112–121. doi: 10.1016/j.msea.2004.05.006
10. J.C. Newman et al., Fatigue and Crack Growth Analysis on Specimens Simulating Details in Wing Panels of Naval Aircraft. *Presentation and in Proceedings, Aging Aircraft Conference*, Phoenix, AZ, 2008,